# Bi-Layer Graphene Nanoribbon Memory with Graphene Nanoflake Shuttle

Oh Kuen Kwon[*], Jeong Won Kang[**] and Jun Ha Lee[***]

[*]Department of Electronic Engineering, Semyung University,
Jecheon 390-711, Republic of Korea, kok1027@semyung.ac.kr
[**]Korea National University of Transportation, Chungju 380-702,
Republic of Korea, jwkang@ut.ac.kr
[***] Department of Computer System Engineering, Sanymyung University,
Chonan 330-720, Republic of Korea, junha@smu.ac.kr

## ABSTRACT

We investigated the dynamic properties of graphene-nanoribbon (GNR) memory encapsulating graphene-nanoflake (GNF) shuttle in the potential to be applicable as a non-volatile random access memory via molecular dynamics simulations. This work explicitly demonstrates that the GNR encapsulating the GNF shuttle can be applied to nonvolatile memory. The potential well was originated by the increase of the attractive vdW energy between the GNRs when the GNF approached the edges of the GNRs. So the bistable positions were located near the edges of the GNRs. Such a nanoelectromechanical non-volatile memory based on graphene is also applicable to the development of switches, sensors, and quantum computing.

***Keywords***: graphene nanoribbon, graphene nanoflake, shuttle memory, molecular dynamics

## 1 INTRODUCTION

Non-volatile random access memory (NVRAM) can retain its information even when not powered. Nowadays, the best-known form of NVRAM is Flash memory. However, with continued scaling down into nanoscale region, Flash memory faces a physical limitation on charge storage in the scaled cell size [1]. Therefore, recently, various NVRAM devices, such as magnetoresistive RAM (MRAM), ferroelectric RAM (FeRAM), phase change RAM (PCRAM) and resistive RAM (RRAM), have been proposed as alternatives with increased capacity [2]. Quite recently, nanoelectromechanical NVRAM using an anchorless design has been presented as one of the shuttle memory [3].

The shuttle memory using carbon nanotube (CNT) was reported at 1999 by Kwon et al. [4] called 'bucky shuttle memory'. Since then, the various types of CNT-based shuttle-memories have been investigated theoretically [5-14]. However, earlier proposals of 'bucky shuttle' memories remain as concepts, due to fabrication difficulty. Quite recently, alternative designs of the shuttle memory based on graphene have been presented in our previous works [15]. For possible schematics of graphene-nanoflake (GNF) shuttle-memory on graphene nanoribbon (GNR), its energetics was investigated via molecular dynamics (MD) simulations [15,16]. The vdW potential energies of GNF on bistable positions were lower than on the others, so it maintained its seat on one of the bistable positions without recharging. When an external force was applied to the GNF, this movable GNF could be shuttled between the bistable states. This proposed GNF shuttle-memory could be nanoscale NVRAM.

However, in the suggested design in our previous works [16], since the GNF was mounting on the GNR without the protection cover, the GNF could be exposed to pollutants or chemicals in the atomosphere, and this can be great drawback in device reliability [17]. So we presented upgrade schematics of the GNF shuttle memory as shown in Figure 1 [17]. Bilayer GNR includes a GNF, and the GNF can be stabilized in one of local energy minima positions. However, our previous work addressed only the simple schematics and basic operation [17]. So in this work, we investigate the operational properties of this proposed device in detail via classical MD simulations. The bistability of the GNF shuttle encapsulated in bilayer GNR could be achieved from the increase of the attractive vdW energy between the GNRs when the GNF approached the edges of the GNRs. This result showed the potential application of the nanoelectromechanical GNR memory as a NVRAM.

## 2 SIMULATION METHODS

Figure 1 shows two states to store binary data, which is fundamentally related to the position of the GNF shuttle encapsulating the bilayer GNR (GNF@GNR). To investigate the dynamic behaviors of the nanoelectromechanical GNR memory, we perform classical MD simulations using the model structure as shown in Figure. 1, which is composed of 1466 carbon atoms; i.e. the GNF is composed of 166 atoms with 1.97 nm × 1.99 nm size, and each of both GNRs is composed of 650 atoms with the length of 7.85 nm [17]. We used an in-house MD code that has been used in our previous works [18-22], via the velocity Verlet algorithm, a Gunsteren–Berendsen thermostat to control the temperature, and neighbor lists to improve the computing performance. The MD time step was $5\times10^{-4}$ ps. We assigned the initial atomic velocities to a

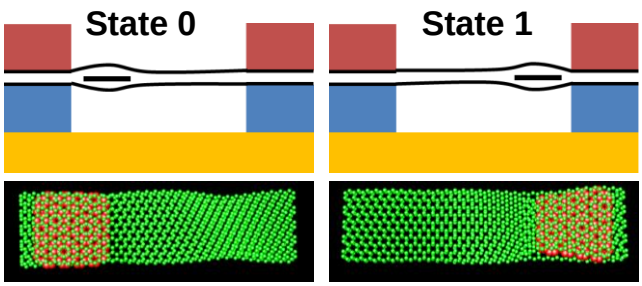


Figure 1: Two states to store binary data.

Maxwell distribution, and the magnitudes were adjusted, in order to fit the temperature of the system. For all MD simulations, the temperature was set to 1 K. Since the both sides of bi-layer GNR are embedded in the electrodes as shown in Figure 1, both edge atoms of the GNRs were fixed during the MD simulations while the GNF shuttle could move freely within bi-layer GNR. First, the GNF was relaxed, without an external force on the GNR. Optimal atomic configurations were obtained using simulated annealing method. To obtain the interatomic energy, we implemented both the Tersoff-Brenner potential [23,24], describing the interactions between carbon atoms that form the covalent bonds of graphene and the Lennard-Jones 12-6 (LJ12-6) potential, describing the long range interactions of carbon. For the LJ12-6 potential, we used the parameters that were given by Mao et al. [25], of $\varepsilon$ = 4.2 meV and $\sigma$ = 3.37 Å , and the cutoff distance was 10 Å .

## 3 RESULTS AND DISCUSSION

Figure 2 shows the parameters related to the operation of the shuttle memory when the force field ($F_A$) of 2 meV/Å was applied to the GNF. The position ($X_S$) of the shuttle was initially around –3 nm (state 0), but the shuttle changed its position around 3 nm (state 1) after 0.01 ns. In other words, the originally stable configuration became unstable in the externally applied force, then, the GNF overcame the potential energy barrier and escaped from the left position, and finally then moved toward the other state. After a few rebounds, the GNF was stabilized. This shuttle memory has a potential to work a NVRAM based on graphene.

The total potential energy ($U$) can be expressed as

$$U = U_C + U_{vdW}, \quad (1)$$

where $U_C$ and $U_{vdW}$ are the covalent bonding and the vdW energies, respectively. In this model system, the $U_{vdW}$ includes the vdW energies of the GNR-GNR and GNR-GNF as follows

$$U_{vdW} = U_{BT} + U_{BS} + U_{TS}, \quad (2)$$

where $U_{BT}$, $U_{BS}$, and $U_{TS}$ are the vdW energies between the GNRs, between the bottom GNR and the GNF, and

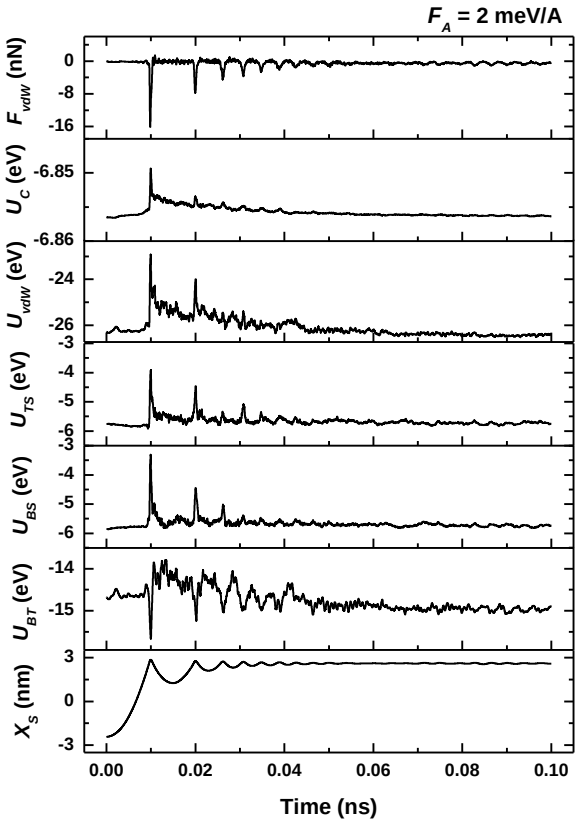


Figure 2: MD results as a function of the MD time when the force field ($F_A$) of 2 meV/Å was applied to the GNF. From bottom, the shuttle's position ($X_S$), the vdW energy between the GNRs ($U_{BT}$), the vdW energy between the bottom GNR and the GNF ($U_{BS}$), the vdW energy between the top GNR and the GNF ($U_{TS}$), the total vdW energy ($U_{vdW}$), the covalent bonding energy per atom ($U_C$), and the vdW force exerted on the GNF along the GNR's axis ($F_{vdW}$).

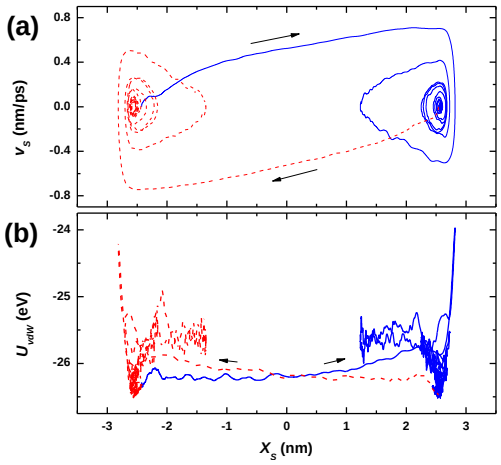


Figure 3: Variations of (a) the shuttle's velocity ($v_S$) and (b) the vdW energy as a function of the shuttle's position ($X_S$) for two cases such as the transition from 'state 0' to 'state 1' under $F_A$ = 2 meV/Å and vice versa under $F_A$ = –2 meV/Å .

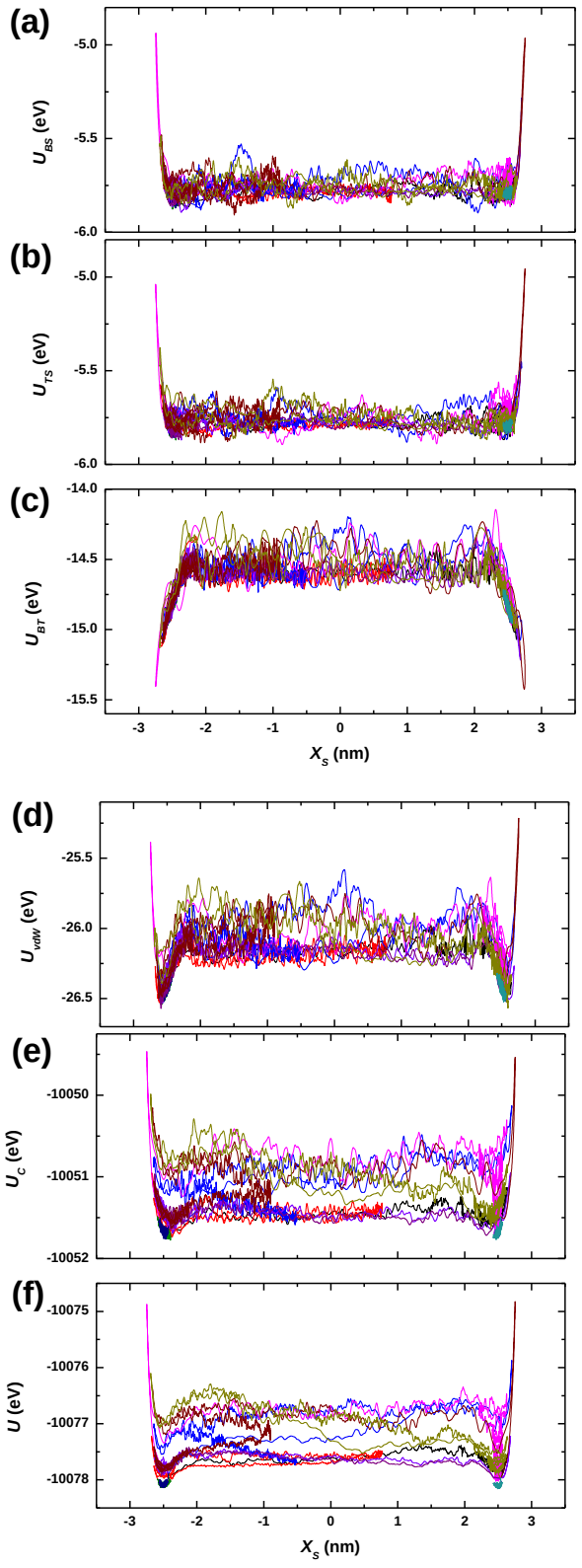


Figure 4: Variations of (a) $U_{BS}$, (b) $U_{TS}$, (c) $U_{BT}$, (d) $U_{vdW}$, (e) $U_C$, and (f) $U$ as a function of the $X_S$ twelve MD simulations with different initial positions and force fields.

between the top GNR and the GNF, respectively. The variations of these potential energies and the vdW force ($F_{vdW}$) exerted on the GNF along the GNR's axis are plotted in Figure 2. During this switching process, the kinetic energy of the GNF gradually increased. However, when the GNF was rebound, some of the kinetic energy was dissipated into heat, and converted into the rotation energy of the GNF, so as a result the GNF was stabilized in the position of 'state 1'. These phenomena can be observed by the variations of the potential energies in Figure 2.

Figures 3(a) and 3(b) show the variations of the shuttle's velocity ($v_S$) and vdW energy as a function of the shuttle's position ($X_S$), respectively, for two cases such as the transition from 'state 0' to 'state 1' under $F_A$ = 2 meV/Å and vice versa under $F_A$ = –2 meV/Å. The $v_S$ - $X_S$ plots in Figure 3(a) show that the momentum of the shuttle converges on the local energy minima positions, which are clearly recognized in the $U_{vdW}$ - $X_S$ plots in Figure 3(b).

The non-volatility of the shuttle memory is closely related to the potential well depth at the local energy minima position. As the potential well depth increases, the non-volatility also increases. So it is very important to know the origin of the potential well. So we performed twelve MD simulations with different initial positions and the force fields, and then we plotted the variations of $U_{BS}$, $U_{TS}$, $U_{BT}$, $U_{vdW}$, $U_C$, and $U$ as a function of the $X_S$ as shown in Figures 4(a)-4(f). When the GNF approached the metal electrodes, the vdW potential energies between the GNF and GNRs abruptly increased as shown in Figures 4(a) and 4(b) whereas the vdW potential energy between the GNRs decreased as a shown in Figure 4(c). Hence, total vdW energy plot, $U_{vdW}$ = $U_{BS}$ + $U_{TS}$ + $U_{BT}$, makes bi-stable potential wells at both edges of the GNRs as shown in Figure 4(d). The potential well was originated by the increase of the attractive vdW energy between the GNRs when the GNF deviated from the center of the GNRs. In other words, the deformations of the GNRs due to the GNF decreased when the GNF was near the edges of GNRs. Therefore, since both $U_{vdW}$ and $U_C$ plots show the local energy minima positions when the GNF shuttle approaches the fixed edges of the GNRs, the total potential energy, $U$ = $U_{vdW}$ + $U_C$, at these positions is minimized. The switching processes via the position change of the GNF can be achieved from various methods such as electrostatic force [26,27], magnetic force, electromigration, or diffusion [28,29]. The stored data can be read by detecting the polarity of the GNF@GNR, using electric, magnetic, or optical methods [16]. This work explicitly demonstrates that the GNF@GNR system can be applied to alternative NVRAM and high speed mass storage by using GNR arrays.

To improve the reliability of the GNF shuttle, firstly the thermal stability of the GNFs should be ensured. Barnard and Snook [30] explored the thermal stability of GNFs by *ab initio* quantum mechanical techniques, and found that indeed GNFs were stable to being heating and did not under any conditions used there transform to CNTs. However, we should note that Chuvilin et al. [31] observed the fullerene

formation directly from graphene while exposed to an 80-keV electron beam (e-beam). Second, the fluctuations of the GNRs as the thermal effects due to the temperature definitely affect the performance of the GNF shuttle encapsulated in GNRs. However, since in this work, all the MD simulations were performed at extremely low temperature, which is very different from the ordinary conditions for experiments or measurements, we should note that the results in this work were restricted in ideal situations. So since it is very important to estimate the temperature range that this electromechanical NVRAM based on GNR memory can be used reliably, thermal effects for the operations of the GNF shuttle should be investigated in further works. Finally, we should note that since the long-range attractive forces [32] between the electrode and the GNF can be influenced on their dynamic properties, these should be also included in further work.

## 4 CONCLUSION

We investigated the dynamic properties of GNR memory encapsulating GNF shuttle in the potential to be applicable as a NVRAM via MD simulations. The simulations results explicitly demonstrated that the GNR encapsulating the GNF shuttle could be applied to nonvolatile memory. Since the potential well was originated by the increase of the attractive vdW energy between the GNRs when the GNF approached the edges of the GNRs, the bistability at the local energy minima positions could be achieved from near the edges of the GNRs. Such a nanoelectromechanical non-volatile memory based on graphene is also applicable to the development of switches, sensors, and quantum computing.

## REFERENCES


[1] C.-H. Cheng, K. I. Chou, Z.-W. Zheng, H.-H. Hsu, Curr. Appl. Phys. **14**, 139 (2014).

[2] Y.-S. Fan, P.-T. Liu, and C.-H. Hsu, Thin Solid Films **549**, 54 (2013).

[3] V. Pott, G. K. Chua, R. Vaddi, J. M.-L. Tsai, and T. T. Kim, IEEE Trans. Electr. Dev. **59**, 1137 (2012).

[4] Y. K. Kwon, D. Tománek, and S. Iijima, Phys. Rev. Lett. **82**, 1470 (1999).

[5] J. W. Kang and H. J. Hwang, Physica E **23**, 36 (2004).

[6] W. Y. Choi, J. W. Kang, and H. J. Hwang, Physica E **23**, 135 (2004).

[7] J. W. Kang and H. J. Hwang, Carbon **42**, 3018 (2004).

[8] J. W. Kang and H. J. Hwang, J. Phys. Soc. Jpn **73**, 1077 (2004).

[9] J. W. Kang. W. Y. Choi, and H. J. Hwang, J. Comput. Theor. Nanosci. **1**, 199 (2004).

[10] H. J. Hwang, W. Y. Choi, and J. W. Kang, Comput. Mater. Sci. **33**, 317 (2005).

[11] K. R. Byun, J. W. Kang, and H. J. Hwang, Physica E **28**, 50 (2005).

[12] J. W. Kang and H. J. Hwang, Mater. Sci. Eng. C **25**, 843 (2005).

[13] Y. Chan, R. K. F. Lee, and J. M. Hill, IEEE Trans. Nanotechnol. **10**, 947 (2011).

[14] R. K. F. Lee and J. M. Hill, Mater. Sci. Forum **700**, 85 (2011).

[15] H. J. Hwang and J. W. Kang, Physica E **56**, 17 (2014).

[16] O. K. Kwon, J. Park, and J. W. Kang, Physica E 58, 88 (2014).

[17] J. W. Kang and K.W. Lee, J. Nanosci. Nanotechnol. (2014) in press.

[18] S.-Y. Kim, H. J. Hwang, and J. W. Kang, Phys. Lett. A **377**, 3136 (2013).

[19] O. K Kwon, K.-S. Ki, J. Park, and J. W. Kang, Computat. Mater. Sci. **67**, 329 (2013).

[20] S.- Y. Kim, S.-Y. Cho, J. W. Kang, and O. K. Kwon, Physica E **54**, 118 (2013).

[21] J. W. Kang, J. Comput. Theor. Nanosci. **10**, 1667 (2013).

[22] J. W. Kang and S. Lee, Computat. Mater. Sci. **74**, 107 (2013).

[23] J. Tersoff, Phys. Rev. B **39**, 5566 (1989).

[24] D. W. Brenner, Phys. Rev. B **42**, 9458 (1990).

[25] Z. Mao, A. Garg, and S. B. Sinnott, Nanotechnology **10**, 273 (1999).

[26] I. V. Lebedeva, A. A. Knizhnik, A. M. Popov, Yu. E. Lozovik, and B. V. Potapkin, Phys. Chem. Chem. Phys. **13**, 5687 (2011).

[27] I. V. Lebedeva, A. A. Knizhnik, A. M. Popov, Yu. E. Lozovik, and B. V. Potapkin, Physica E **44**, 949 (2012).

[28] I. V. Lebedeva, A. A. Knizhnik, A. M. Popov, O. V. Ershova, Yu. E. Lozovik, and B. V. Potapkin, Phys. Rev. B **82**, 155460 (2010).

[29] I. V. Lebedeva, A. A. Knizhnik, A. M. Popov, O. V. Ershova, Yu. E. Lozovik, and B.V. Potapkin, J. Chem. Phys. **134**, 104505 (2011).

[30] A. S. Barnard and I. K. Snook, J. Chem. Phys. **128**, 094707 (2008).

[31] A. Chuvilin, U. Kaiser, E. Bichoutskaia, N. A. Besley, and A. N. Khlobystov, Nature Chemistry **2**, 450 (2010).

[32] M. Sakamoto, Y. Kanda, M. Miyahara, and K. Higashitani, Langmuir **18**, 5713 (2002).